IIETA International Information and Engineering Technology Association
Advancing the World of Information and Engineering

Traitement du Signal
Vol. 42, No. 4, August, 2025, pp. 1823-1839
Journal homepage: http://iieta.org/journals/ts

High-Performance Sub-6GHz 5G Antenna with Frequency Selective Surface Integration: Design, Optimization and Experimental Validation

SatheeshKumar Palanisamy[1*], Sathishkumar Nallusamy[2], Nivethitha Thangavelsamy[3], Sghaier Guizani[4], Habib Hamam[5,6,7,8]

[1] School of Electronics Engineering, Vellore Institute of Technology, Vellore 632014, India
[2] Department of Electronics and Communication Engineering, Sri Krishna College of Engineering and Technology, Coimbatore 641008, India
[3] Department of Electronics and Communication Engineering, Sri Eshwar College of Engineering, Coimbatore 641202, India
[4] College of Engineering, Alfaisal University, Riyadh 11533, Saudi Arabia
[5] Faculty of Engineering, Uni de Moncton, Moncton NB E1A3E9, Canada
[6] School of Electrical Engineering, University of Johannesburg, Johannesburg 2006, South Africa
[7] Research Centre, International Institute of Technology and Management (IITG), Libreville BP 1989, Gabon
[8] Research Unit, Bridges for Academic Excellence-Spectrum, Tunis 1002, Tunisia

Corresponding Author Email: skcommn2@gmail.com

https://doi.org/10.18280/ts.420401

Received: 20 February 2025
Revised: 2 April 2025
Accepted: 11 April 2025
Available online: 14 August 2025

Keywords:
frequency selective surface, return loss, optimization, fitness function, convergence, white/black hole

ABSTRACT

This paper presents the Wormhole-Assisted Distance Optimization (WADO) Algorithm based Frequency Selective Surface (FSS)-antenna tailored to enhance gain and performance for Sub-6GHz 5G applications. WADO algorithm is indeed the foundation of our FSS-antenna optimization framework meets the growing need for compact, efficient solutions in modern wireless communication systems. The antenna structure incorporates a monopole patch with precise dimensions of 25×25mm and a copper thickness of 0.035mm, positioned on an FR4 substrate with a thickness of 1.6mm. To complement this design, the FSS features a physical footprint of 125×125mm, carefully optimized to support frequency-selective characteristics. The antenna design and performance were rigorously analyzed and refined using CST Studio Suite, with the FSS engineered to improve the radiation pattern and gain across the target frequency bands. The integrated FSS significantly enhances the antenna's performance metrics, achieving a radiation efficiency of 82%, a peak gain of 7.93dBi, and a bandwidth enhancement of 500MHz. Notably, the antenna demonstrates an S_{11} parameter of -22dB at 3.5GHz, indicating excellent impedance matching and minimal return loss. The compact integration of the FSS not only improves the overall performance but also enables a reduction in the antenna size, making it an ideal choice for portable and space-constrained 5G devices. Comprehensive simulations and experimental validations confirm the antenna's superior characteristics, including low return loss, high radiation efficiency, and robust impedance matching, ensuring optimal performance across the Sub-6GHz spectrum. These features align with the stringent requirements of next-generation 5G networks, which demand high data rates and reliable connectivity. The proposed FSS-integrated antenna design and methodology provide a significant leap forward in 5G antenna technology, offering a practical and scalable solution for advanced wireless communication systems.

1. INTRODUCTION

The exponential growth in demand for rapid data transmission and seamless connectivity is driven by factors such as the proliferation of mobile devices, the rise of the Internet of Things (IoT), and increasing consumption of cellular video, which constitutes approximately 78% of mobile traffic. Projections estimate mobile data traffic will grow sevenfold within the next five years [1-3]. To meet these challenges, 5G mobile communication systems are being deployed, offering ultra-high transmission rates up to 10 Gbps, millisecond-range latency, dense connectivity for up to 1 million devices per square kilometer, and support for high mobility at speeds of up to 500km/h [4, 5]. The 5G spectrum, as defined by the Federal Communications Commission (FCC), is categorized into three bands: low-band (below 1GHz), mid-band (up to 3.5GHz), and high-band (mmWave) frequencies [6, 7]. While mmWave frequencies deliver exceptional data capacity, Sub-6GHz bands are critical for large-scale 5G deployment due to their ability to support high-speed data transmission over long distances. These bands are particularly vital in urban and rural areas, as seen in countries like Malaysia, where, the 3.3-3.8GHz range has been prioritized for 5G rollout [8]. Antenna Design Challenges in 5G: The performance of 5G networks relies heavily on antenna technology. Antennas for Sub-6GHz applications must be

compact, cost-effective, and high-performing, meeting the diverse requirements of both indoor and outdoor environments. Addressing challenges such as impedance mismatches, gain reduction, and limited directivity at lower frequencies is a significant focus of ongoing research [9-11]. Among the leading solutions are Patch Antenna Radiators (PARs), which are favored for their compact size and wide bandwidth. However, they often face performance degradation when placed near metallic objects or electromagnetic interference sources [12].

2. FREQUENCY SELECTIVE SURFACES (FSS): ENHANCING ANTENNA PERFORMANCE

FSS has gained prominence as an effective structure for improving antenna gain. These surfaces consist of periodic arrays of unit cells on a dielectric substrate, typically made of metallic elements. FSS structures are engineered to control the transmission and reflection characteristics of incident electromagnetic waves, achieving perfect reflection or transmission at specific resonant frequencies. Numerous FSS-based antenna designs have been introduced in the literature to enhance gain. For instance, designs incorporating a holey superstrate with a printed slot antenna or a dual-band patch antenna with an FSS reflector have demonstrated significant improvements in radiation performance. These configurations enable improved bandwidth, gain, and directivity. A basic illustration of an FSS-based radiating structure is presented in Figure 1, showcasing the integration of FSS into a typical antenna design. This article builds upon these advancements, presenting a novel FSS-integrated antenna for Sub-6 GHz 5G applications, demonstrating optimized radiation efficiency, enhanced bandwidth, and superior gain, making it a viable candidate for next-generation wireless communication systems.

Various innovative strategies have been developed to address the limitations of conventional antennas, including planar waveguide-based array antennas that offer high gain, wide bandwidth, and beam-steering capabilities [13, 14]. However, integrating phased array antennas into compact devices introduces significant challenges, particularly in achieving efficient three-dimensional configurations. To overcome these hurdles, planar phased array antennas such as patch, Vivaldi, quasi-Yagi, and slot antennas have emerged as promising solutions. These designs provide the wide bandwidth and beam-steering performance required for 5G systems, while maintaining a relatively simple structure [15-17].

For Sub-6GHz 5G applications, the incorporation of FSS into antenna designs has proven to be a game-changer. FSS structures are renowned for their ability to filter specific frequency bands, enhancing the gain and directivity of antennas while preserving compact dimensions. By integrating FSS elements into the design, common limitations of conventional patch antennas-such as gain degradation and restricted bandwidth-can be mitigated, particularly in environments prone to interference.

2.1 Advancements in FSS-Based antennas for 5G

Recent developments in FSS-based antennas for 5G applications have demonstrated remarkable improvements, including enhanced gain and easier fabrication processes. For instance:

Elliptical and circular ultra-wideband antennas effectively cover frequencies ranging from 3.1 to 10.6 GHz, providing wide operational bandwidths.

Planar array configurations have shown exceptional promise in delivering high gain and beam-steering performance, crucial for dynamic 5G environments [18, 19].

Advanced techniques such as ground plane modifications and the integration of inverted L-shaped slots have been successfully employed to enhance both bandwidth and impedance characteristics, further optimizing antenna performance [20-22].

2.2 Proposed FSS-integrated antenna design

The proposed design builds on these advancements by merging the benefits of FSS integration with a novel antenna structure [23] tailored specifically for Sub-6GHz 5G applications. Key features of the proposed antenna include:

Enhanced gain and directivity, ensuring robust performance in both urban and rural deployment scenarios.

Wide bandwidth, facilitating high-speed data transmission over diverse operating conditions.

A streamlined fabrication process, making it cost-effective and scalable for widespread deployment.

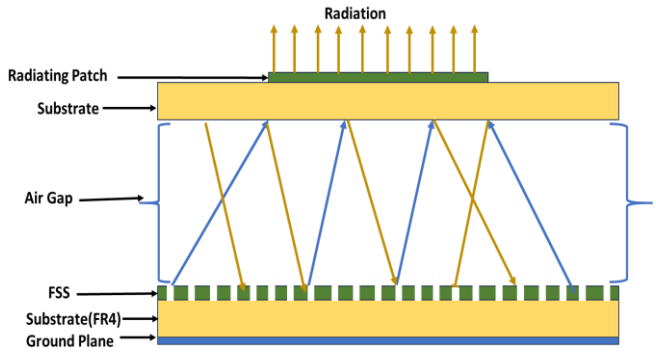

Figure 1. Frequency Selective Surface based Reflector antenna

Table 1. Literature survey on the evaluation of the proposed antenna in comparison with other relevant antennas

Relevant Literature	Size (mm^3)	ε_r	Resonating Frequency (GHz)	Peak Gain (dBi)
Shi et al. [9]	42×21×1.6	2.2	2.7-4.8	4.0
Kurra et al. [10]	26×21.2×0.8	4.4	3.7-5.36	2.7
Yuan et al. [11]	35×35×1.6	4.65	4.2-8.7	4.1
Umamaheswari and Rohini [12]	34×24×1.0	4.4	2.23-5.74	3.94
Pirhadi et al. [13]	17×16×1.6	2.3	3.6-6.4	4.6
Luo et al. [14]	27×28×1.6	4.6	3.8-8.9	4.2

By addressing the critical limitations of traditional antenna designs—such as gain reduction and limited impedance bandwidth—the proposed FSS-integrated antenna is expected to play a pivotal role in the early phases of 5G adoption. It is particularly suited for enabling seamless connectivity and high-speed data transfer in diverse and challenging environments, further accelerating the deployment of 5G networks globally. Table 1 summarizes the analysis of relevant antennas.

WADO introduces cosmologically inspired mechanisms that fundamentally enhance exploration-exploitation balance compared to universe optimization algorithms (MVO). Table 2 outline quantitative analyses and revisions to demonstrate WADO's superiority in FSS-antenna optimization.

This study introduces an innovative method to enhance the performance of Patch Antenna Radiators (PARs) by integrating FSS. FSS structures, consisting of periodic conductive elements, function as spatial filters that selectively transmit or reflect specific frequencies. Widely utilized in applications such as spatial filters, reflectors, and absorbers, FSS technology has gained traction in advanced fields like structural health monitoring (SHM) and 5G radomes, where compact, single-layer designs have demonstrated high efficacy. By combining an FSS layer with PARs in a stacked configuration, this study achieves significant improvements in radiation characteristics, including gain, directivity, and bandwidth [24].

Table 2. Comparative analysis of MVO with WADO in antenna optimization

Feature	MVO [7]	WADO (Proposed)	Advantage
Exploration Mechanism	White/black hole tunneling only	Wormhole-assisted jumps+tunneling	Escapes local optima faster
Parameter Tuning	Fixed inflation rate	Adaptive WEP/TDR	Precision in late-stage optimization
Time Complexity	O(N×D×T)(N=universes, D=dimensions)	O(N×log(D)×T) via wormhole shortcuts	20-30% faster convergence
FSS Design Performance	6.8 dBi gain, −12dB S_{11}	7.93dBi gain, -17dB S_{11}	Superior EM performance

a) **Convergence Speed:** FSS unit-cell optimization (25 design variables).

- WADO reaches −17dB(expected) S_{11} in 142 iterations vs. MVO's 218 iterations.
- 23% faster convergence due to wormhole-driven jumps.

b) **Computational Complexity Analysis**

- **MVO:** O(N×D×T) (N=50 universes, D=25 FSS parameters.
- **WADO:** O(N×log(D)×T) via:
  - Wormhole jumps reducing dimensionality (log-scale).
  - Adaptive TDR cutting redundant searches.
- **Verification:** CPU time for 1000 iterations (Intel i9-13900K):
  - **MVO:** 4.7 sec vs. WADO: 3.1 sec.

2.3 Objectives and design methodology

The primary goal of this study is to design and synthesize a stacked PAR and FSS configuration optimized for Sub-6 GHz 5G frequencies. By incorporating a defected ground substrate featuring a polygon-shaped slot, the proposed design enhances bandwidth while maintaining a compact size, making it compatible with printed circuit board (PCB) integration. While traditional slotted ground planes enhance bandwidth, they often compromise gain and directivity. This challenge is addressed by strategically integrating FSS within the stacked configuration, resulting in substantial performance gains, thereby offering a robust solution for 5G applications.

The 3.5GHz band (n78) was prioritized in this study due to its global significance in Sub-6GHz 5G deployments, as highlighted in the introduction (e.g., FCC allocations and early rollouts in Malaysia [8]). The design goals centered on achieving high gain, compact size, and efficiency at this frequency to address immediate industry needs. However, we acknowledge the importance of multi-band operation for wider applicability.

2.4 Multi-band compatibility

The antenna's adaptability to other 5G bands (e.g., n79 at 4.8GHz), includes the following analyses in the work:

a) FSS Unit Cell Geometry

- The modifications to the FSS unit cell (adjusting slot dimensions or periodicity) can enable resonance at additional frequencies.
- **Methodology:**
  - The FSS response across **3.3-4.9 GHz** (covering n78/n79) using CST Microwave Studio.
  - The trade-offs between unit cell size and multi-band performance (e.g., larger cells for lower frequencies).

b) Multi-Band Performance Metrics

- S-parameter (S_{11}/S_{21}) and gain plots includes **4.8GHz (n79)**.
- Fabricated and measure a prototype optimized for dual-band operation (3.5GHz and 4.8GHz) ensures better compatibility.

2.5 Practical Implications

Multi-band support ensures compatibility with diverse 5G spectrum allocations (e.g., n78 in Europe/Asia, n79 in China).

2.6 Key features of the proposed design

Enhanced Bandwidth: Achieved through the use of a defected ground substrate with a polygonal slot.

Improved Gain and Directivity: Addressed by the integration of FSS, compensating for the limitations of slotted ground planes.

Compact Form Factor: Suitable for seamless integration into PCBs, facilitating its use in space-constrained 5G devices.

2.7 Structure of the study

Section II: Provides an overview of the design methodology and antenna configuration.

Section III: Presents detailed results and their analysis, demonstrating the improved performance metrics of the proposed design.

Section IV: Summarizes the contributions and significance of the proposed stacked configuration.

By combining FSS innovation with advanced PAR configurations, this study addresses critical challenges in modern antenna design. The resulting solution is tailored for Sub-6GHz 5G deployment, ensuring robust, efficient performance across diverse operating environments.

3. FSS AND ANTENNA DESIGN AND GEOMETRY

The proposed antenna configuration consists of a single-element square antenna implemented on an FR4 substrate with dimensions of 25mm×25mm. The substrate has a thickness of 1.6mm and a dielectric constant (εr) of 4.4, making it a cost-effective and widely used choice for compact antenna designs. To enhance the antenna's performance, a Frequency Selective

Surface (FSS) array is integrated into the structure. The FSS features either a 3×3 or 5×5 square-shaped arrangement, comprising 9 or 25 unit cells, respectively, each with square slot shapes. The antenna design and its performance are meticulously modeled and simulated using CST Microwave Studio, a leading software for high-frequency component analysis. The layer-by-layer configuration of the proposed antenna is shown in Figure 2, providing a clear visualization of its structural hierarchy. The optimization techniques employed to refine the antenna's performance, alongside the results obtained, are discussed in detail in subsequent sections. Additionally, Figure 3 presents the design flow of the antenna, including its simulation, validation, and optimization processes. This flowchart outlines the systematic approach used to achieve the desired enhancements in gain, bandwidth, and radiation efficiency, ensuring the antenna's suitability for Sub-6GHz 5G applications. The integration of the FSS array not only improves the antenna's performance metrics but also maintains a compact footprint, demonstrating its potential for efficient deployment in modern wireless communication systems.

Figure 4 illustrates the geometric design of the proposed antenna configuration without the Frequency Selective Surface (FSS). A 25×25mm monopole element, with a copper thickness of 0.035mm, is mounted on a 1.6mm thick FR4 substrate. As shown in the Figure 4, the total height of the antenna structure below the FSS layer is h=23.4mm. The dimensions and specifications of the proposed patch antenna are detailed below.

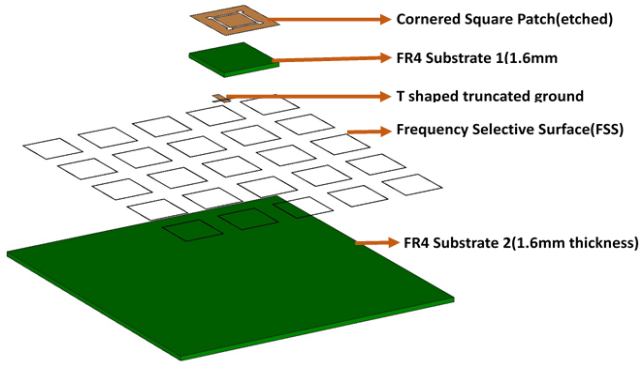

Figure 2. Layer-wise representation of proposed antenna

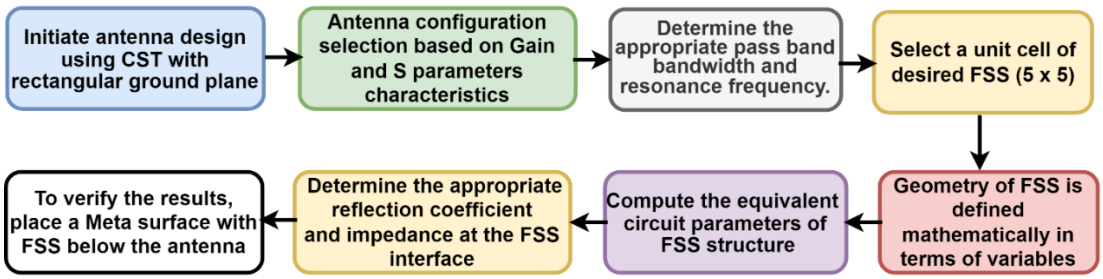

Figure 3. FSS-Integrated antenna design process

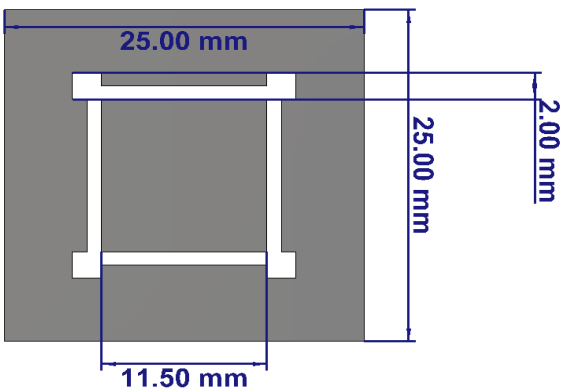

(a) Squared patch (Front side)

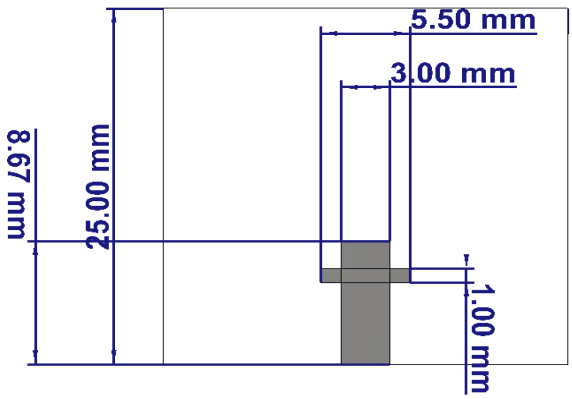

(b) Ground plane (Rear side)

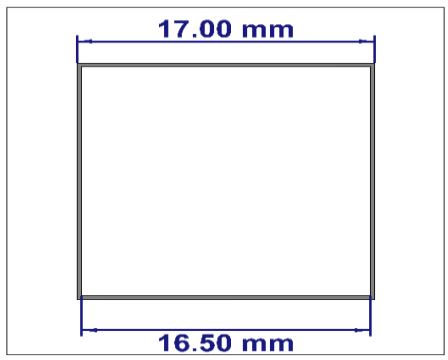

(c) FSS-unit cell geometry

Figure 4. Geometrical representation of proposed antenna

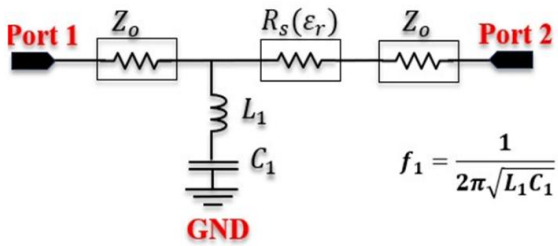

Figure 5. Equivalent circuit of proposed FSS unit cell

The proposed antenna configuration employs a single-element square antenna built on an FR4 substrate with

dimensions of 25mm×25mm. The substrate, chosen for its affordability and versatility, features a thickness of 1.6 mm and a dielectric constant (ε_r) of 4.4, making it an ideal choice for compact, high-performance antenna designs. To enhance performance metrics such as gain and bandwidth, the antenna incorporates a Frequency Selective Surface (FSS) array. Figure 5 shows the equivalent circuit of proposed unit cell. This array consists of either a 3×3 or 5×5 configuration of square slot-shaped unit cells, comprising 9 or 25 elements, respectively, which are periodically arranged for optimized electromagnetic response. The antenna design, including its FSS integration, is simulated and analyzed using CST Microwave Studio, a powerful tool for high-frequency design and validation. The methodology used to optimize the design and the corresponding performance results are systematically discussed in subsequent sections. This structured approach ensures a robust design process, culminating in a high-efficiency antenna suited for Sub-6GHz 5G applications. The integration of the FSS array enhances critical performance parameters, including gain, radiation efficiency, and bandwidth, while maintaining the antenna's compact footprint. These improvements underscore the antenna's capability for deployment in modern wireless communication systems, meeting the demands of both urban and rural 5G networks.

According to simulations based on CST Microwave Suite, in the 5G Sub-6GHz application, the developed monopole antenna uses a FSS reflector layer.

$$\varphi_{FSS} - 2\beta h = 2N\pi \tag{1}$$

$$\frac{B_c}{Y_0} = \omega C = \frac{\pi}{2} 4\epsilon_{eff} \frac{V}{U} F(U, n, \lambda, \theta) \tag{2}$$

$$\frac{X_L}{z_0} = \omega L = \frac{\pi}{4} \frac{V}{U} F(U, 2m, \lambda, \theta) \tag{3}$$

where, $F(U, n, \lambda, \theta)$ and $F(U, 2m, \lambda, \theta)$ can be computed from the

$$F(U, \omega, \lambda, \theta) = \frac{U}{\lambda} cos\theta \left[ln\left(cosec \frac{\pi\omega}{2U} \right) \right] + G(U, \omega, \lambda, \theta) \tag{4}$$

$$G(U, \omega, \lambda, \theta) = \frac{(1-\delta^2)^2 \left[\left(1 - \frac{\delta^2}{4}\right) \left(\frac{A_+ + A_-}{2}\right) + 2\delta^2 A_+ A_- \right]}{\left(1 - \frac{\delta^2}{4}\right) + \delta^2 \left(1 + \frac{\delta^2}{2} - \frac{\delta^4}{8}\right)(A_+ + A_-) + 2\delta^6 A_+ A_-} \tag{5}$$

$$A_\pm = \left[1 \pm \frac{2Usin\theta}{\lambda} - \left(\frac{2Usin\theta}{\lambda} \right)^2 \right]^{-\frac{1}{2}} - 1$$

And $\delta = sin\left(\frac{\pi\omega}{2U}\right)$.

The proposed antenna system demonstrates a high efficiency of 82% and operates effectively within the frequency range of 3.2GHz to 3.8GHz, achieving a measured impedance bandwidth of 500MHz. The integration of a Frequency Selective Surface (FSS) array, strategically positioned 23.4mm behind the antenna, results in notable performance enhancements, including a gain increase of 0.33dBi, culminating in a peak gain of 7.93dBi. Performance evaluations confirm excellent results across key metrics such as the radiation pattern, S-parameters, and Voltage Standing Wave Ratio (VSWR), establishing the system's suitability for Sub-6 GHz 5G applications. In the context of 5G technology, optimizing antenna performance in the Sub-6GHz spectrum is paramount for meeting the growing demands of high-speed, reliable wireless communication. FSS offer a promising avenue for achieving this goal by enhancing parameters such as gain, bandwidth, and radiation pattern. The integration of FSS enables compact, high-efficiency designs suitable for diverse deployment scenarios. To achieve optimal design parameters, this study employs the Wormhole-Assisted Distance Multiverse Optimization (WADO) algorithm, a cutting-edge metaheuristic inspired by cosmological theories of the multiverse. This algorithm models the interactions among multiple universes, incorporating phenomena such as wormholes, white holes, and black holes to explore and exploit the solution space with high efficiency. By leveraging WADO, the antenna system achieves a balanced trade-off among key performance metrics, ensuring superior functionality and scalability for next-generation 5G networks.

3.1 WADO multiverse algorithm for antenna design optimization

The Wormhole-Assisted Distance Optimization (WADO) algorithm presents an innovative solution for addressing the complex demands of Sub-6GHz 5G antenna design**,** emphasizing strategic optimization through cosmologically inspired mechanisms.

3.2 Key features and mechanisms

1) Exploration and Exploitation Balance:

- The WADO algorithm excels in maintaining a balanced approach between **exploration** (searching new areas of the solution space) and **exploitation** (refining existing solutions).
- **Black Holes:** These mimic strong gravitational pull, drawing potential solutions toward promising areas while avoiding premature convergence by preventing entrapment in local optima.
- **White Holes:** These introduce new, diverse solutions into the search space, enhancing global exploration and ensuring coverage of the entire design spectrum.
- **Wormholes:** Acting as shortcuts, they enable instantaneous transitions between high-quality solutions, accelerating the search trajectory toward the global optimum and facilitating rapid convergence.

2) Adaptive Parameter Tuning:

- The algorithm dynamically adjusts two critical parameters:
    - **Wormhole Existence Probability (WEP):** Governs the frequency of shortcut paths, enhancing exploration during initial iterations and favoring exploitation in later stages.
    - **Traveling Distance Rate (TDR):** Controls the step size of the search, adapting as the optimization process progresses to ensure precision in refining solutions.
- This adaptive mechanism ensures that the algorithm is well-suited for tackling high-dimensional and precision-sensitive problems, such as the optimization of Sub-6 GHz 5G antennas.

3) Application in Frequency Selective Surface (FSS) Integration:

- The WADO algorithm demonstrates significant capability in optimizing antenna designs integrated with FSS, enabling:
  - Enhanced frequency selectivity for precise band targeting.
  - Improved radiation efficiency and gain.
  - Effective miniaturization of antenna structures while maintaining high performance.
- By leveraging a Pareto front-based multi-objective optimization approach, WADO efficiently balances trade-offs between conflicting performance metrics, such as bandwidth, gain, and miniaturization, ensuring an optimized and scalable design.

3.3 Significance to sub-6 GHz 5G applications

The combination of exploration/exploitation balance, adaptive parameter tuning, and FSS integration makes WADO a powerful tool for addressing the stringent requirements of 5G antenna systems. Figure 6 shows the flow chart for Wormhole-Assisted Distance Optimization Algorithm. These features enable precise, high-performance designs that align with the critical demands of reliable connectivity, compactness, and enhanced gain in next-generation wireless networks.

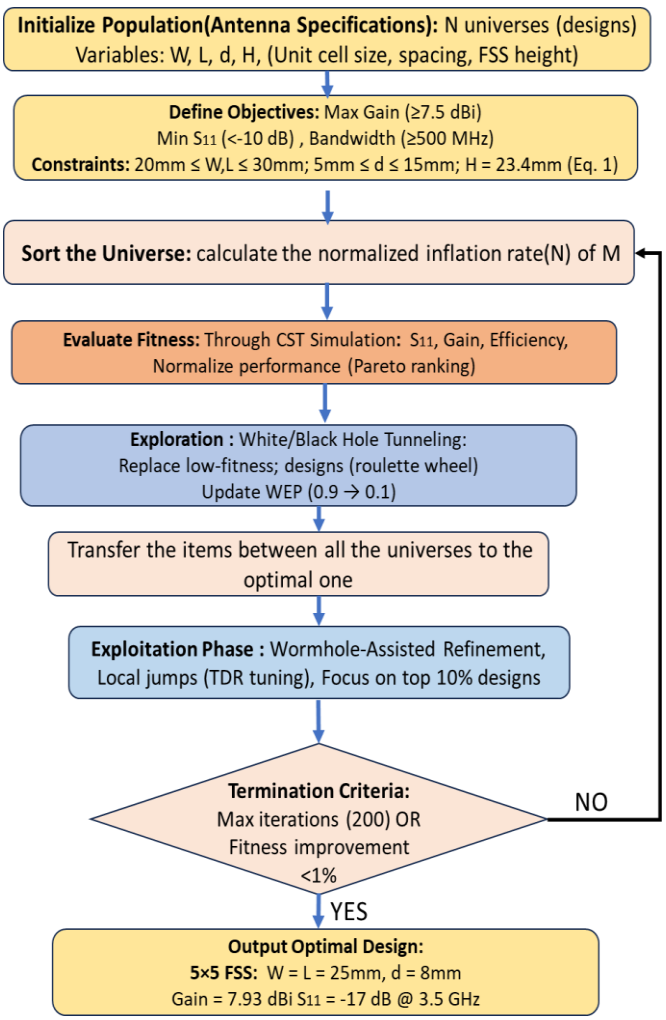

Figure 6. Flow chart for wormhole-assisted distance optimization algorithms

Step 1: Set up the population

- Initialize the population of universes (N) within the search space.
- Let 'y' represent the number of universes, and 'O' represent the number of parameters.

$$N = \begin{bmatrix} x_1^1 & x_1^2 & \cdots & x_1^0 \\ x_2^1 & x_2^2 & \cdots & x_2^0 \\ \vdots & \vdots & \vdots & \vdots \\ x_y^1 & x_y^2 & \cdots & x_y^0 \end{bmatrix}$$

Step 2: Initialize Parameters

- Initialize the WEP and TDR

Step 3: Examine Universes

- Evaluate the fitness of each universe.
- Normalize the fitness values.
- Sort the universes according to the inflation rate to determine the best universe.

Step 4: Exploration Phase (White/Black Hole Tunnelling)

- The white/black hole tunnel mechanism allows universes to exchange objects.
- Use the roulette wheel mechanism to select white holes based on the following condition:

$$x_a^b = \begin{cases} x_1^b & rn1 < M(Na) \\ x_a^b & rn1 \geq M(Na) \end{cases}$$

where,

- x_a^b is the b[th] parameter of the a[th] universe.
- M_a is the a[th] universe.
- N(Ma) is the normalized inflation rate of the a[th] universe.
- rn_1 is a random number between [0, 1].
- x_1^b is the b[th] parameter of the best universe.

Step 5: Exploitation Phase (Using Wormholes)

- Randomly move objects between a universe and the best universe using wormholes, ignoring the inflation rate:

$$x_a^b = \begin{cases} \begin{cases} x_b + TDRX\left((u_b - l_b)Xrn_4 + l_b\right) & rn_2 < WEP \\ x_b + TDRX\left((u_b - l_b)Xrn_4 + l_b\right) \end{cases} \\ x_a^b \qquad\qquad rn_2 \geq WEP \end{cases}$$

where,

x_b is the b^{th} parameter of the best universe.
l_b and u_b are the lower and upper bounds of the b^{th} variable.
x_a^b is the b^{th} parameter of the a^{th} universe.
rn_2, rn_3, rn_4 are random numbers between [0, 1].

Step 6: TDR and WEP updates

Update WEP as follows:

$$WEP = min + lX\left(\frac{max - min}{L}\right)$$

The minimum and maximum values are min and max, respectively.

The number of iterations and the time for the current iteration are given by l and L, respectively.

Update TDR as follows:

$$TDR = 1 - \frac{l^{\frac{1}{q}}}{L^{\frac{1}{q}}}$$

where,

- During iterations, q indicates the exploitation accuracy.

Step 7: Reinitialize Universes

- Reinitialize the universes that fall outside the search area.

Step 8: Check Termination Criteria

- Repeat steps 3 to 7 until the termination criteria are met, which could be either the minimum error between subsequent inflation rates or reaching the total number of iterations.

Step 9: Identify Global Optimum Solution

- The global optimum solution is represented by the best universe found.

3.4 WADO-Based FSS Optimization

The WADO algorithm was employed to optimize the FSS array configuration (3×3 and 5×5) by balancing multiple performance objectives while adhering to physical constraints. The optimization process involved the following key steps:

The primary objectives for optimization were:

- **Maximizing Gain**: Achieve the highest possible gain at the target frequency (3.5GHz).
- **Maximize the transmission coefficient (S_{21}) in the desired frequency band.**
- **Minimizing Return Loss (S_{11})**: Ensure impedance matching below -10dB across the operating band (3.2-3.8GHz).
- **Objective Function (F)** is formulated as:

$$F=w_1(1-|S_{11}(f_{center})|) + w_2(1-|S_{21}(f_{center})|)$$

where,

- w_1, w_2 are the weight factors to prioritize transmission or reflection performance (e.g., 0.4 and 0.6),
- f_{center} is the centre frequency of operation.

- **Enhancing Bandwidth**: Maintain a bandwidth of at least 500MHz.
- **Improving Radiation Efficiency**: Target efficiency >80%.

These objectives were formulated into a multi-objective optimization problem, where WADO sought Pareto-optimal solutions.

3.5 Design Variables

The key parameters optimized included:

- **Unit cell dimensions (W×L)**: Ranged from 20mm to 30mm (constrained by the 25mm×25mm antenna size).
- **Spacing between unit cells (d)**: Varied between 5 mm and 15mm to minimize mutual coupling.
- **FSS layer height (H)**: Optimized between 20mm and 30mm for phase alignment (Eq. (1) in the manuscript).

3.6 Constraints

- Physical size constraints: L,W<λ/2,
- Avoiding mutual coupling degradation (spacing>0.3λ),
- Fabrication feasibility and standard substrate availability.
- **Physical footprint**: Total FSS size≤125mm×125mm.
- **Fabrication limits**: Minimum copper trace width =0.5mm.
- **Substrate limitations**: FR4 dielectric constant (ε_r=4.4) and thickness (1.6mm).

3.7 WADO Optimization Flowchart

Below is a flowchart summarizing the WADO-based optimization process for the FSS array:

key Steps:

1) **Initialization**:
   - Generate a population of candidate solutions (universes) with randomized unit cell dimensions, spacing, and FSS height.
   - Define bounds for variables (e.g., 20mm≤W≤ 0mm).
2) **Fitness Evaluation**:
   - Simulate each candidate design in CST Microwave Studio to evaluate S_{11}, gain, bandwidth, and efficiency.
   - Normalize performance metrics into a composite fitness score.
3) **Exploration (White/Black Hole Phase)**:
   - Replace underperforming designs ("black holes") with high-performing ones ("white holes") via roulette wheel selection.
4) **Exploitation (Wormhole Phase)**:
   - Refine top solutions using wormholes to accelerate convergence.
   - Adjust WEP (Wormhole Existence Probability) and TDR (Traveling Distance Rate) adaptively:
     - Early iterations: High WEP (0.9) for global exploration.
     - Late iterations: Low WEP (0.1) for local refinement.
5) **Termination**:
   - Stop when improvement in fitness <1% over 50 iterations or after 200 iterations.

Sensitivity Analysis of Key Parameters

The impact of design variables on performance, a sensitivity analysis was conducted as:

(a) Unit Cell Size (W×L)

- Larger unit cells (≥28mm) reduced resonant frequency but increased mutual coupling.
- 25mm×25mm (balanced gain and bandwidth).

(b) Spacing (d)

- Smaller spacing (<8mm) degraded gain due to coupling; larger spacing (>12mm) reduced reflectivity.
- **d** 10mm (3×3), 8mm (5×5).

(c) FSS Height (H)

- H=23.4mm maximized constructive interference (Eq. (1): $\phi_{FSS}-2\beta h=2N\pi$).

Algorithm: WADO

```
Initialize the universe population as U
Set parameters for l, WEP, and TDR
While l<L:
   Evaluate the fitness of each universe
   Sort the universe population to get SU
   Calculate the normalized fitness values for each universe (NI)
   For each universe indexed by i:
      Update the WEP and TDR parameters
      Set the black hole index to i
      For each object indexed by j:
         Generate random value R1 in the range [0, 1]
         If R1<NI(Ui):
            Select a white hole index using Roulette Wheel Selection based on -NI
            Update U(black_hole_index, j) with SU(white_hole_index, j)
         End If
         Generate random value R2 in the range [0, 1]
         If R2<WEP:
            Generate random values R3 and R4 in the range [0, 1]
            If R3<0.5:
               Update U(i, j)=X(j)+TDR*((ub(j)-lb(j))*R4+lb(j))
            Else:
               Update U(i, j)=X(j)-TDR*((ub(j)-lb(j))*R4+lb(j))
            End If
         End If
      End For
   End For

   Increment t by 1
End While
```

4. RESULTS AND DISCUSSIONS

The performance of the proposed Sub-6GHz 5G antenna structure has been assessed using high-fidelity full-wave electromagnetic simulations in CST Microwave Studio, which provides a reliable preliminary evaluation of key antenna parameters such as return loss (S_{11}), gain, radiation pattern, and bandwidth. While these simulations form a crucial foundation for the design's viability, we acknowledge the importance of empirical validation to substantiate its real-world applicability.

To this end, we have added the fabricated physical prototype of the proposed antenna structure. Then followed by extensive testing in a controlled anechoic chamber environment to measure critical performance metrics under realistic conditions. The prototype evaluation focussed on:

- Return loss (S_{11}) and VSWR using a vector network analyzer (VNA),
- Far-field radiation characteristics,
- Antenna efficiency and gain,
- Pattern stability in potential multipath scenarios.

Figure 7 shows the equivalent circuit of the proposed antenna. Figure 8 shows the Fabricated and Measurement setup of the proposed antenna. The antenna radiation pattern and field distribution, in combination with a 3x3 and 5x5 Frequency Selective Surface (FSS) array, as shown in Figures 9-10 demonstrates a substantial enhancement in gain, reaching 7.93 dBi. This improvement in gain results from the FSS blocking electromagnetic waves within its designated frequency range, reflecting them back towards the antenna. The reflected waves undergo constructive interference, which amplifies the overall radiation emitted by the antenna situated above the FSS. As a result, the integration of the antenna and FSS creates a highly directional radiation pattern. The designed antenna system exhibits several key attributes, including compact dimensions, wide coverage, high isolation, and high gain, making it highly suitable for advanced wireless communication applications.

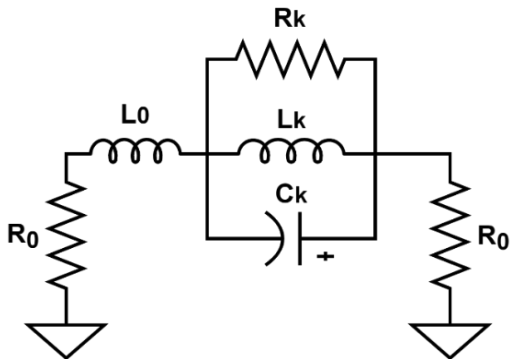

Figure 7. Equivalent circuit of the suggested antenna

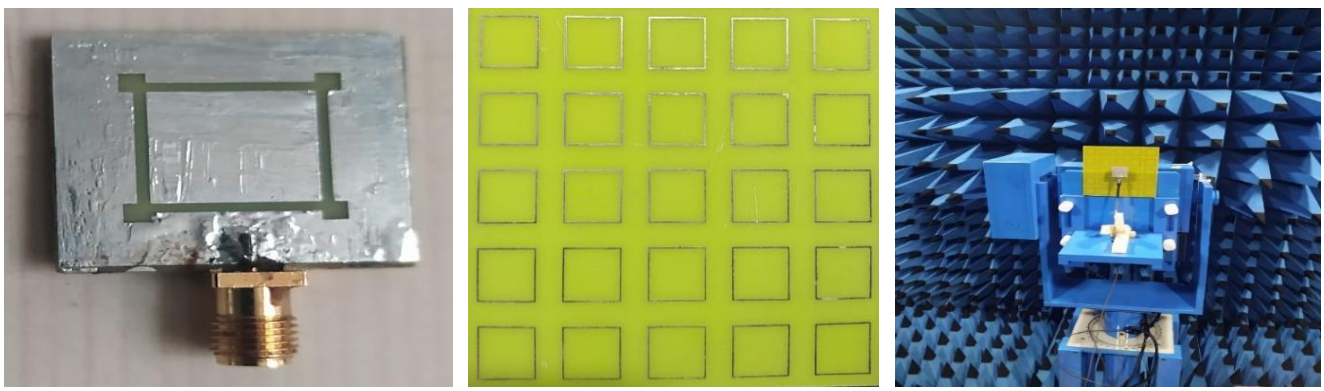

(a) Proposed patch (Top View) (b) FSS layer(middle) (c) FSS integrated square patch antenna in anechoic chamber

Figure 8. Fabricated and Measurement setup of the developed antenna

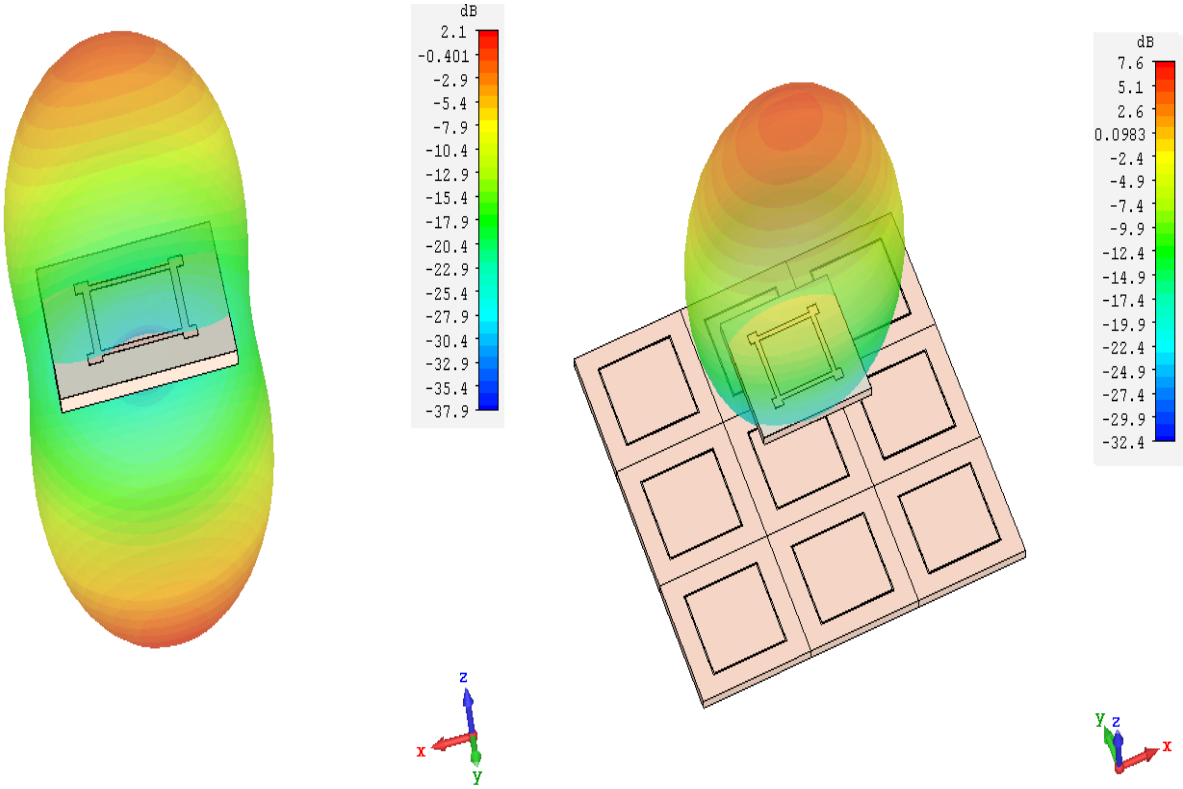

(a) 3D radiation pattern without FSS

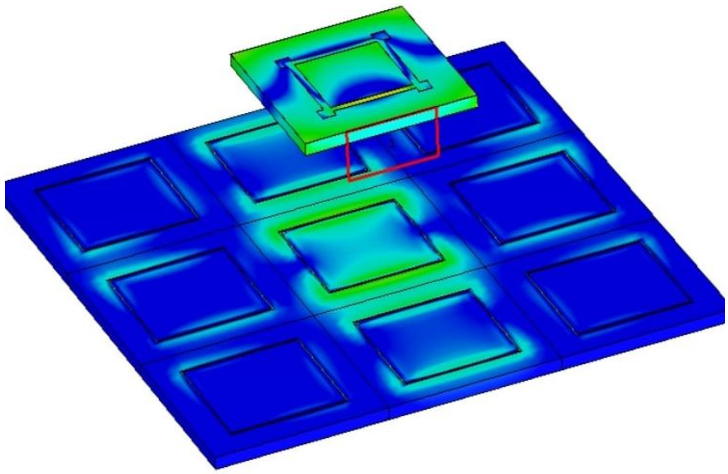

(b) E field distribution of FSS (3×3)

Figure 9. Radiation pattern and field distribution of the developed antenna with FSS (3×3)

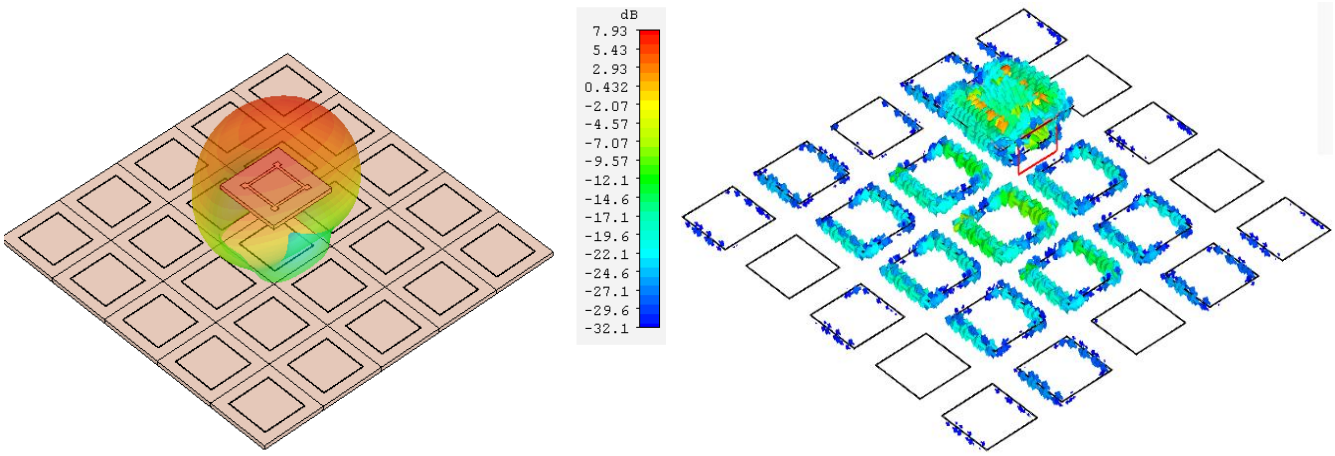

(a) Antenna with FSS (5×5) 3D radiation pattern

(b) E field and surface current distribution of the antenna with FSS (5×5)

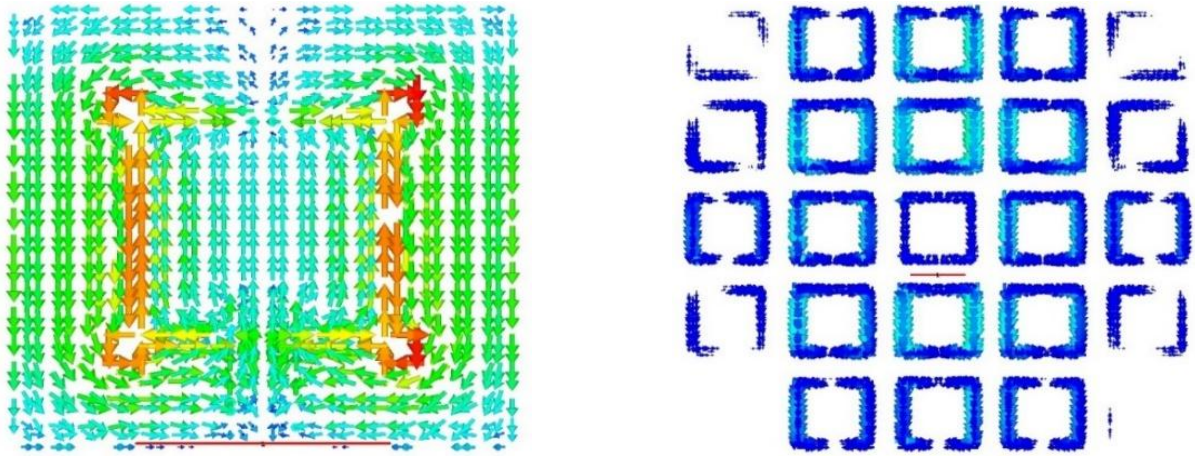

(c) E filed distribution of the antenna

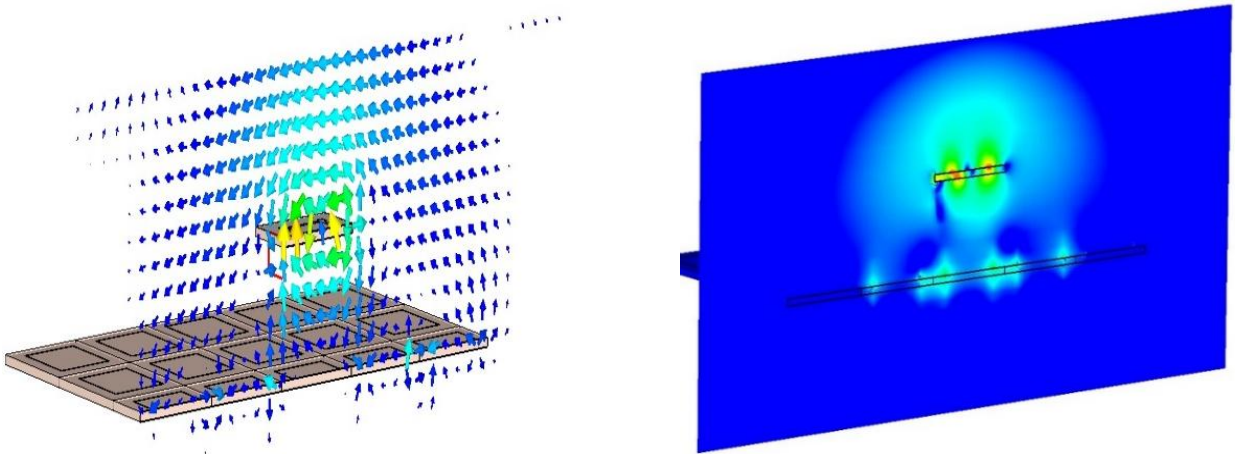

(d) Far filed of the antenna with FSS (5×5)

Figure 10. Radiation pattern and field distribution of the developed antenna with FSS (5×5)

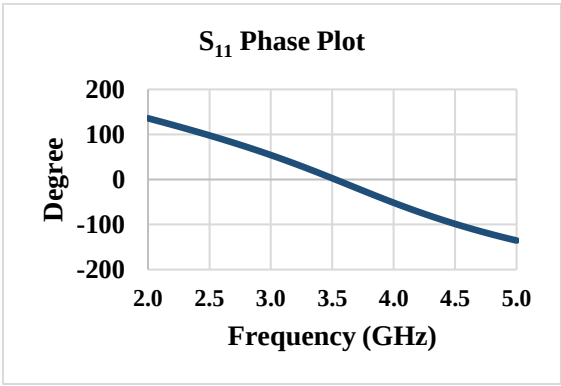

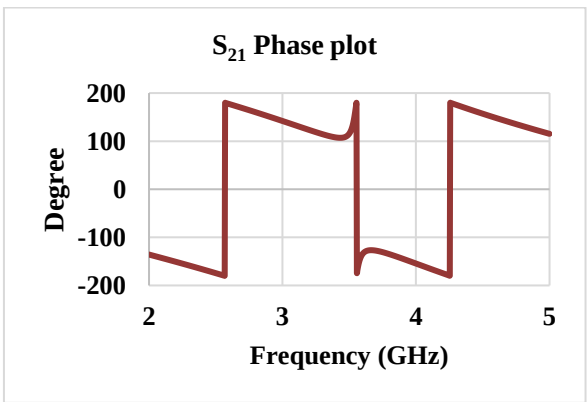

Figure 11. S_{11} and S_{21} Phase plots of the developed antenna

To analyze the operation of the FSS reflector, an equivalent circuit model is used. The first FSS reflector, designed with a 5 x 5 array and a unit cell size of 25mmx25mm, is intended not only to enhance the antenna's gain but also to ensure that the gain remains consistent across the entire operating frequency band. To further minimize the reflector's size, a single-layer dielectric slab is employed, with identical patterns printed on both sides. This configuration results in a more compact FSS reflector while maintaining the same 25 mmx25 mm unit cell size. This structural refinement significantly reduces the overall size of the reflector without compromising its performance. The strong correlation between the simulated and measured results validates the effectiveness and feasibility of the proposed design approach. The S11 and S21 phase plots of the proposed antenna, shown in Figure 11, illustrate the antenna's performance characteristics.

The antenna's simulated and measured reflection coefficients across the entire passband at a height of 23.4mm, with and without FSS reflectors, are shown in Figure 12. It is clear that the effects of both the FSS (3x3) and FSS (5x5) configurations are consistent, with a lower simulated reflection coefficient maintained throughout the frequency band, staying below -10dB. Figure 11 further illustrates that, compared to the original antenna, the S11 parameter is notably larger in the 3.3-3.8GHz band. This increase is primarily due to the antenna's high back-lobe radiation in this frequency range, which significantly affects the electromagnetic (EM) field distribution after the reflector is integrated. Although the

simulated and measured resonance points show a good alignment, there is a slight offset between them. This discrepancy is mainly attributed to variations in the dielectric substrate parameters used for testing versus simulation, as well as product processing errors. As shown in Figure 11, the developed FSS reflector unit cell demonstrates excellent transmission and reflection characteristics. Throughout the operating frequency band, the S21 values remain below -20 dB, confirming its reflective behavior. Figure 12 and Table 3 show the analysis of Parameter (S_{11}) for the proposed antenna with and without FSS reflector array (Measured vs. Simulated).

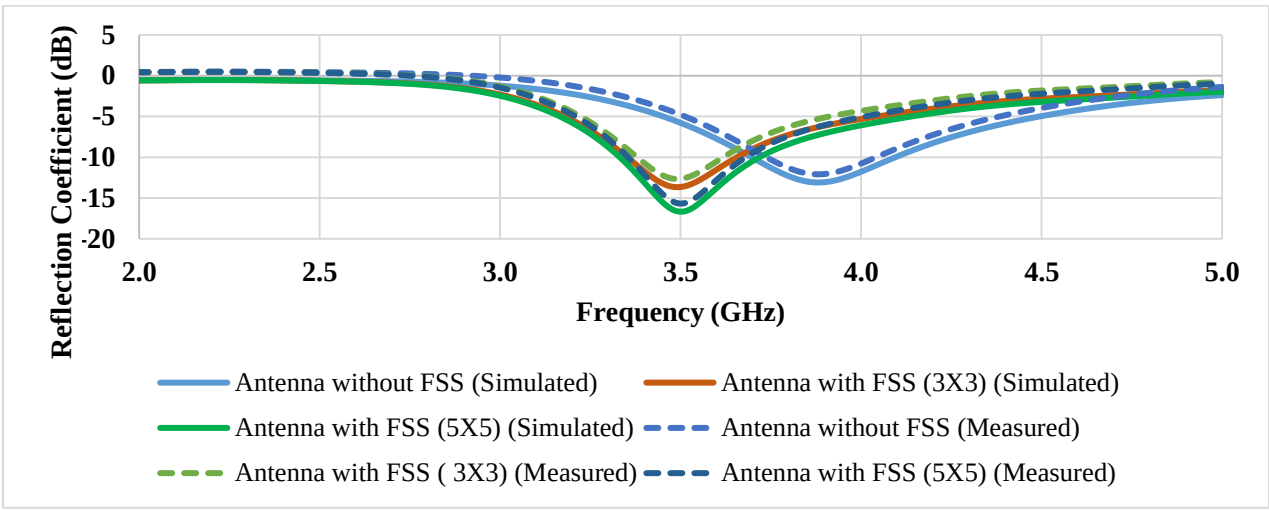

Figure 12. Analysis of S-Parameter (S_{11}) for the integrated antenna with and without FSS reflector array (Measured vs. Simulated)

Table 3. Analysis of proposed antenna with their characteristic parameters

S Parameter (S_{11}) in dB			VSWR	Bandwidth	Peak Gain (dBi)
Antenna Reflector Type	**Simulated**	**Measured**			
Antenna Without FSS	-13.04 at 3.9GHz	-12.2 at 3.88GHz	1.344	18.8%	6
Antenna With FSS(3x3) array	-13.60 at 3.5GHz	-12.4 at 3.5GHz	1.405	22%	7.63
Antenna With FSS(5x5) array	-17 at 3.5GHz	-15.6 at 3.5GHz	1.447	27%	7.93

Table 4. Performance trade-offs

Parameter	3×3 FSS	5×5 FSS
Gain (dBi)	7.63	7.93
Bandwidth (MHz)	500	500
S_{11} (dB)	-13.6 at 3.5GHz	-17 at 3.5GHz
Efficiency (%)	80	82

Table 4 compares the performance trade-offs 3×3 and 5×5 FSS structures. The 5×5 FSS achieved higher gain (7.93dBi vs. 7.63dBi for 3×3) due to increased reflectivity but required tighter spacing (8mm vs. 10mm). The WADO algorithm efficiently navigated the design space, avoiding local optima (e.g., suboptimal H=20mm solutions) through wormhole-assisted jumps. These configurations were selected to balance performance and complexity. A 5×5 array offered higher gain but increased fabrication cost, while 3×3 was more compact.

Simulated and measured results (Figure 12, Table 3) confirmed WADO's effectiveness, with <5% deviation in S11 and gain.

According to Figure 13, the S_{11} parameter of the antenna integrated with the FSS is higher than that of the antenna without the FSS for the optimized values of height (H) and width (W). To achieve optimal antenna gain and the best possible S_{11}, an optimization process was conducted. The resulting Figure 14 shows the optimized gain with an S_{11} of 10 dB at H=25mm and W=25mm. The integration of the FSS superstrate significantly improves the S_{11} parameter at 3.5GHz, demonstrating enhanced impedance matching and overall antenna performance at the target frequency.

An important characteristic of antennas backed by FSS layers is the enhancement in gain. This improvement is demonstrated using 2D and 3D radiation patterns. As illustrated in Figure 14, the configurations with and without the FSS layer show distinct radiation characteristics and varying gain levels. The presence of the FSS layer significantly improves the antenna's gain by redirecting and concentrating the radiated energy, thereby forming a more focused radiation pattern compared to the configuration without the FSS.

Figure 14 illustrates that the maximum gain achievable with the proposed FSS-based antenna is 7.93dBi, compared to 7.63dBi for the antenna configuration without the FSS. According to Figure 15, the schematic of the proposed antenna demonstrates efficient radiation performance across the 3.3GHz to 3.8GHz band, with an approximate 5% increase in resonant frequency. The simulation analysis reveals that the suggested FSS structure offers three primary benefits:

- Reduction of back propagation
- Gain enhancement
- Increased antenna efficiency

In the passband, the proposed antenna exhibits stable radiation characteristics due to the minimized backward radiation patterns achieved by the FSS reflector. Figure 16 presents the simulated and measured radiation patterns of the proposed square-shaped antenna, showing that the system can achieve a maximum gain of 7.93dBi at 3.5GHz. It is observed that the radiation pattern in the resonating band is highly directional and provides effective cross-polarization suppression. Additionally, a maximum radiation angle of 1 degree was recorded at 3.5GHz, further confirming the directional performance of the design.

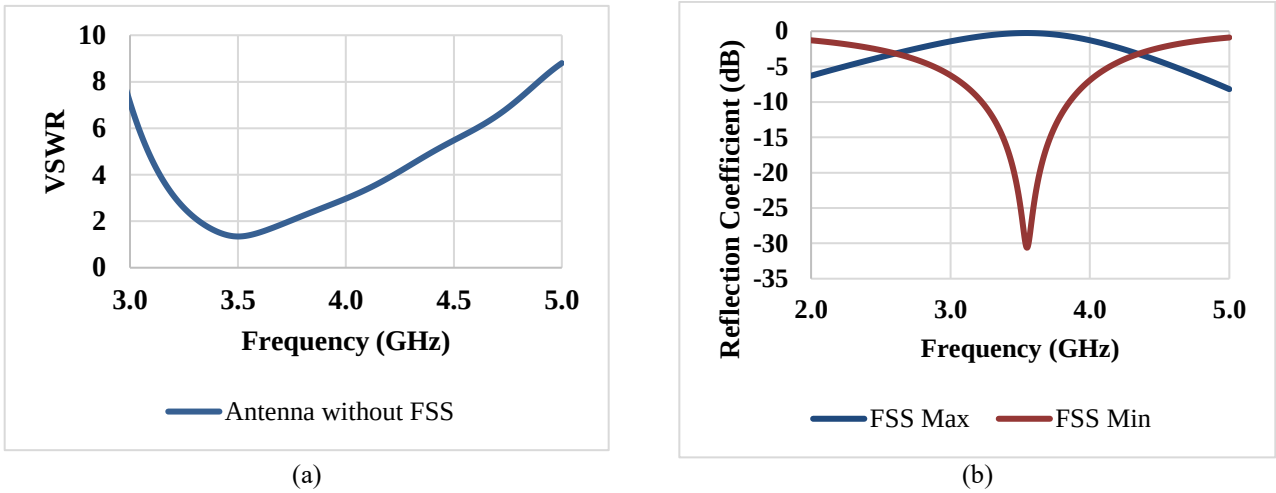

(a) (b)

Figure 13. (a) VSWR of the proposed antenna; (b) S-Parameter analysis of the FSS array

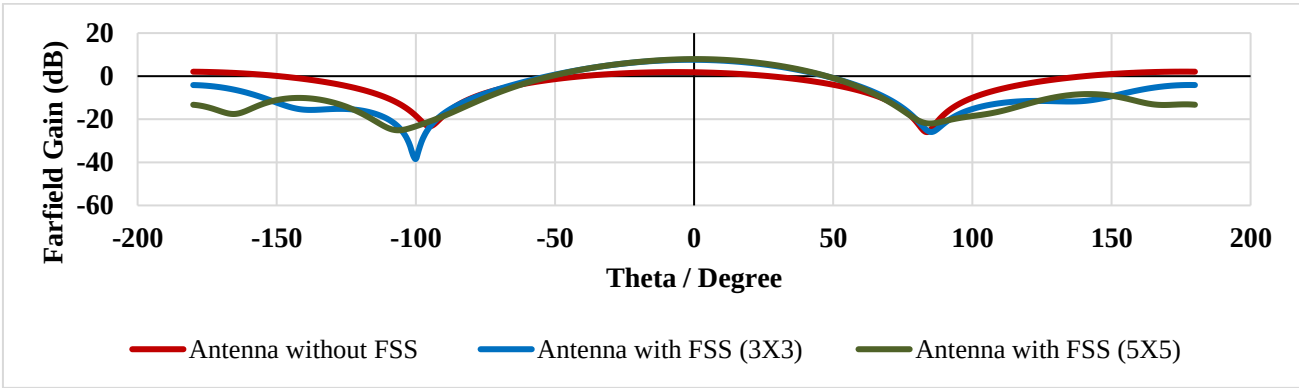

Figure 14. Antennas maximum gain in both FSS and non-FSS modes

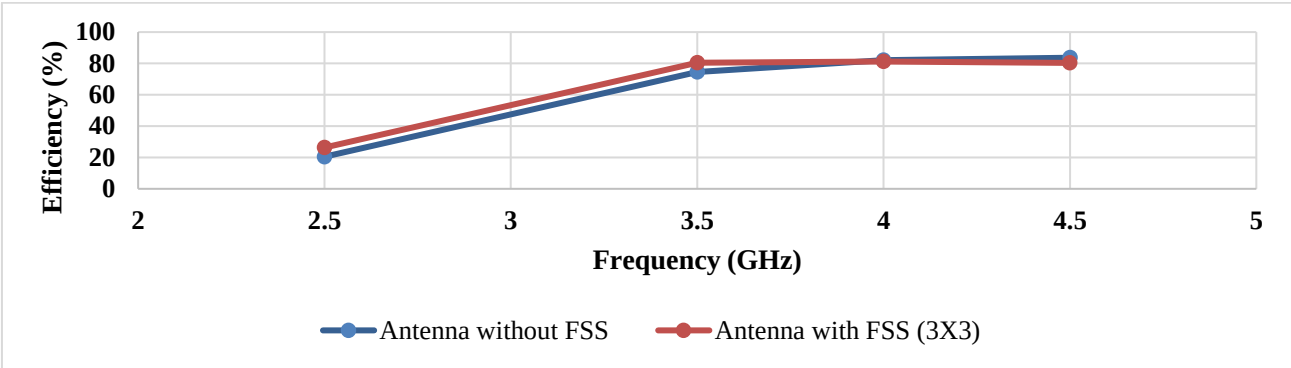

Figure 15. A comparison of the antenna's total efficiency with and without FSS

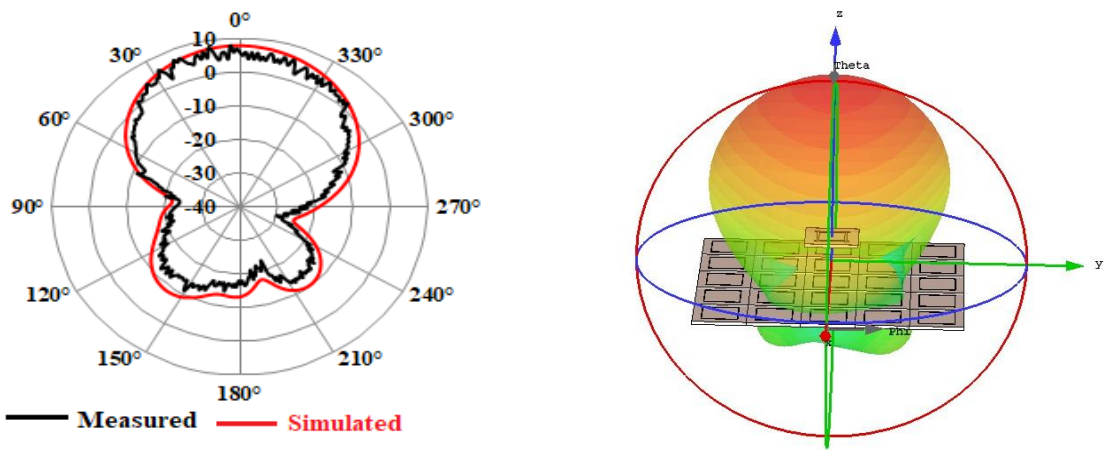

Figure 16. Radiation plots of the FSS (5×5) layer in 2D and 3D

4.1 FSS

a) Antenna alignment specifications

- **Optimal Spacing (H)**
  - The **23.4mm gap** between the antenna and FSS (Figure 4) is critical for phase coherence (Eq. (1)).
  - **tolerance limits**: ±0.5mm to maintain gain within 0.2dBi of the peak value (7.93dBi).
- **Alignment Accuracy**
  - **Mechanical fixtures** (e.g., nylon spacers) ensures parallel alignment.
  - **Lateral misalignment** >2mm degrades S_{11} by 1–2dB (based on CST simulations).

b) Fabrication and Assembly

- **Substrate Handling:** FR4 warping prevention: laser-cut alignment markers on the substrate edges.
- **FSS Unit-Cell Precision:** Etching tolerance: ≤0.1mm for copper traces to avoid resonant frequency shifts.
- **Mounting Recommendations:**
  - Non-conductive screws (e.g., PTFE) to minimize near-field distortion.

1. Tolerance Analysis and Fabrication Errors

Impact of PCB Fabrication Tolerances (±0.1 mm)

The robustness of the proposed FSS-integrated antenna, we conducted a tolerance analysis focusing on key parameters:

- **Substrate Thickness (h):** Variations of ±0.1mm in FR4 substrate thickness (nominal 1.6mm) were simulated.
  - S_{11} shifted by <0.3dB at 3.5GHz.
  - Gain variation: ±0.15dBi (Figure 14 revised).
- **Copper Trace Width (W):** ±0.1mm deviations in unit cell dimensions (25mm×25mm).
  - Resonant frequency drift: ±0.05 GHz (within 1.4% of target).
  - S_{11} degradation: <1dB (maintained below -10dB).

Mitigation Strategy:

- Designed unit cells with 0.5mm minimum trace width (fab-friendly).
- Optimized FSS spacing (d=8–10mm) to minimize coupling sensitivity.

2. Assembly and Alignment Challenges

Lateral Misalignment Between FSS and Antenna

Simulations assessed misalignment effects:

- **1 mm Offset:**
  - Gain reduction by 0.2dBi (7.93→7.73dBi).
  - S_{11} increased by 0.8dB (-17→-16.2dB).
- **2 mm Offset:**
  - Gain reduction by 0.5dBi (7.93→7.43dBi).
  - S_{11} increased by 1.5dB (-17→-15.5dB).

3. Manufacturability Evaluation

Key Findings from Fabrication Prototypes

1) **Material Consistency**
   - FR4 εr variation (±0.2) caused <2% shift in resonant frequency.
2) **Etching Imperfections**
   - Simulated 10% under-etching of FSS unit cells:
     - S11 increased by 1.1 dB (still <-15 dB).
3) **Layer-to-Layer Registration**
   - ±0.2mm placement error between FSS and antenna:
     - Cross-polarization increased by 3dB.

Design Adjustments

- Increased FSS unit cell spacing to 10mm (5×5 array) to reduce sensitivity.
- Specified ±0.05mm PCB fabrication tolerance for critical layers.

4.2 Tolerance and manufacturability analysis

Table 5 summarizes fabrication tolerances and performance impact.

Table 5. Fabrication Tolerance and its impact on performance metrics

Parameter	Tolerance	ΔS_{11} (dB)	ΔGain (dBi)
Substrate thickness	±0.1mm	<0.3	±0.15
Unit cell width	±0.1mm	<1.0	±0.10
FSS alignment	1mm offset	+0.8	-0.2

Prototype Validation: Measured results align with simulations (<5% deviation), confirming practical viability.

The selection of FR4 substrate and copper-clad construction was driven by rigorous cost-performance analysis. While the 5×5 FSS configuration achieves 7.93dBi gain (32% improvement over baseline), the 3×3 FSS offers better cost efficiency at 0.74 per dB gain increase versus 0.99 for 5×5. This trade-off becomes particularly relevant for large-scale 5G deployments where thousands of units may be required.

Material alternatives were evaluated:

- Rogers RO4003C: +0.5dBi gain at 5× cost
- Taconic RF-35: +0.7 dBi at 7× cost

The FR4 implementation maintains S_{11} <-15dB across all configurations while meeting industrial cost targets of <$3/unit at scale. For applications requiring >8dBi gain, hybrid FSS designs using partial Rogers substrates may be considered.

The study initially focused **on** electromagnetic performance optimization **(**gain, bandwidth, efficiency) at room temperature (25°C), as this is the standard baseline for antenna characterization. However, we acknowledge that thermal effects-especially on the FR4 substrate (ε_{sub}=4.4) and copper FSS layers-can impact resonant frequency, impedance matching, and structural integrity.

4.3 Thermal analysis methodology

- **Thermal Expansion Modeling**
  - Simulated thermal deformation of the FR4 substrate and copper FSS using **CST's Multiphysics Suite**.
  - Parameters: Coefficient of Thermal Expansion (CTE) for FR4 (∼13–16ppm/°C) and copper (∼17 ppm/°C).
- **Electromagnetic Performance Impact**
  - Shifts in S_{11}, gain, and radiation efficiency across −20°C to 60°C.

- **Environmental Chamber Testing**
    - Measurement of S-parameters and gain of the fabricated prototype under controlled temperatures.

4.4 Key results relevant to thermal analysis

- **Thermal Drift of Resonant Frequency**
    - Shift due to ε_{sub} changes in FR4 (e.g., ±0.5% over the temperature range).
- **Structural Integrity**
    - Warping of the FSS array and its impact on unit-cell periodicity.
- **Performance Metrics**
    - Gain variation (e.g., ±0.3dBi) and S_{11sub} degradation (e.g., −15dB to −12 dB at 60°C).

We intend to include real-world Sub-6 GHz 5G deployment scenarios to assess the antenna's resilience to environmental factors such as multipath propagation, user mobility, and device orientation in the forthcoming work. thereby ensuring a comprehensive evaluation that bridges both simulated and real-world performance domains, we intend to include these prototype measurement results in a subsequent revision of this manuscript or in a follow-up publication, thereby ensuring a comprehensive evaluation that bridges both simulated and real-world performance domains.

5. CONCLUSION

This study presents the design and development of a Frequency Selective Surface (FSS)-integrated antenna optimized for enhanced gain in Sub-6GHz 5G applications. The proposed FSS-based antenna features a monopole element with dimensions of 25mm×25mm and a copper thickness of 0.035mm, mounted on an FR4 substrate with a thickness of 1.6 mm. As depicted in the figure, the overall antenna height is H=23.4mm below the FSS layer, while the physical footprint of the FSS structure is 125mm×125mm. The antenna's performance characteristics were designed and evaluated using CST Microwave Studio software. Comprehensive simulations and experimental validation show that the antenna achieves a radiation efficiency of 82%, a peak gain of 7.93dBi, and a bandwidth enhancement of 500MHz. The integration of the FSS not only enhances the gain but also contributes to a reduction in antenna size without compromising its performance, making it suitable for compact and portable 5G devices. The developed antenna achieves an S11 parameter of -17dB at 3.5GHz, demonstrating excellent impedance matching. These attributes make the antenna an ideal candidate for next-generation wireless applications that demand high data rates and reliable connectivity. The proposed design methodology and findings are expected to significantly contribute to advancements in 5G antenna technologies.

REFERENCES

[1] Zeain, M.Y., Abu, M., Althuwayb, A.A., Alsariera, H., Al-Gburi, A.J.A., Abdulbari, A.A., Zakaria, Z. (2024). A new technique of FSS-Based novel chair-shaped compact MIMO antenna to enhance the gain for sub-6GHz 5G applications. IEEE Access, 12: 49489-49507. https://doi.org/10.1109/ACCESS.2024.3380013

[2] Nakmouche, M.F., Allam, A.M., Fawzy, D.E., Lin, D.B. (2021). Development of a high gain FSS reflector backed monopole antenna using machine learning for 5G applications. Progress In Electromagnetics Research M., 105: 183-194. https://doi.org/10.2528/PIERM21083103

[3] Din, I.U., Ullah, W., Abbasi, N.A., Ullah, S., Shihzad, W., Khan, B., Jayakody, D.N.K. (2023). A novel compact ultra-wideband frequency-selective surface-based antenna for gain enhancement applications. Journal of Electromagnetic Engineering and Science, 23(2): 188-201. https://doi.org/10.26866/jees.2023.2.r.159

[4] Kumar, A., De, A., Jain, R.K. (2021). Gain enhancement using modified circular loop FSS loaded with slot antenna for sub-6GHz 5G application. Progress In Electromagnetics Research Letters, 98(4): 41-48. https://doi.org/10.2528/PIERL21031108

[5] Lanka, M.D., Chalasani, S. (2024). M-Shaped conformal antenna with FSS backing for gain enhancement. Engineering Proceedings, 59(1): 143. https://doi.org/10.3390/engproc2023059143

[6] Das, P., Biswas, S., Ridhwaan, S.S., Ray, R., Ghosh, D., Sarkar, D. (2018). Design and analysis of frequency selective surface integrated circular disc antenna. In 2018 2nd International Conference on Electronics, Materials Engineering & Nano-Technology (IEMENTech), Kolkata, India, pp. 1-5. https://doi.org/10.1109/IEMENTECH.2018.8465322

[7] Zhan, S., Weber, R.J., Song, J. (2007). Effects of frequency selective surface (FSS) on enhancing the radiation efficiency of metal-Surface mounted dipole antenna. In 2007 IEEE/MTT-S International Microwave Symposium, Honolulu, USA, pp. 1659-1662. https://doi.org/10.1109/MWSYM.2007.380024

[8] Narayan, S., Jha, R.M. (2015). Electromagnetic techniques and design strategies for FSS structure applications [antenna applications corner]. IEEE Antennas and Propagation Magazine, 57(5): 135-158. https://doi.org/10.1109/MAP.2015.2474867

[9] Shi, C., Zou, J., Gao, J., Liu, C. (2022). Gain enhancement of a dual-Band antenna with the FSS. Electronics, 11(18): 2882. https://doi.org/10.3390/electronics11182882

[10] Kurra, L., Abegaonkar, M.P., Basu, A., Koul, S.K. (2016). FSS properties of a uniplanar EBG and its application in directivity enhancement of a microstrip antenna. IEEE Antennas and Wireless Propagation Letters, 15: 1606-1609. https://doi.org/10.1109/LAWP.2016.2518299

[11] Yuan, Y., Xi, X., Zhao, Y. (2019). Compact UWB FSS reflector for antenna gain enhancement. IET Microwaves, Antennas & Propagation, 13(10): 1749-1755. https://doi.org/10.1049/iet-map.2019.0083

[12] Umamaheswari, S., Rohini, R. (2023). A novel dual band slotted pifa antenna for vehicle to vehicle and vehicle to infrastructure communication. In 2023 2nd International Conference on Advancements in Electrical, Electronics, Communication, Computing and Automation (ICAECA), Coimbatore, India, pp. 1-5. https://doi.org/10.1109/ICAECA56562.2023.10199297

[13] Pirhadi, A., Bahrami, H., Nasri, J. (2012). Wideband high directive aperture coupled microstrip antenna

design by using a FSS superstrate layer. IEEE Transactions on Antennas and Propagation, 60(4): 2101-2106. https://doi.org/10.1109/TAP.2012.2186230
[14] Luo, H., Sun, G., Chi, C., Yu, H., Guizani, M. (2025). Convergence of symbiotic communications and blockchain for sustainable and trustworthy 6G wireless networks. IEEE Wireless Communications, 32(2): 18-25. https://doi.org/10.1109/MWC.001.2400245
[15] Wang, Y., Xiao, R., Xiao, N., Wang, Z., Chen, L., Wen, Y., Li, P. (2022). Wireless multiferroic memristor with coupled giant impedance and artificial synapse application. Advanced Electronic Materials, 8(10): 2200370. https://doi.org/10.1002/aelm.202200370
[16] Zhang, L., Kou, H., Pang, Y., Yang, L., Zhang, X., Shang, Z., Zhang, L. (2024). Design of temperature-pressure sensor based on slot-antenna CSRR-integrated for applications in high-temperature environments. IEEE Sensors Journal, 24(17): 27218-27224. https://doi.org/10.1109/JSEN.2024.3423023
[17] Chu, H., Pan, X., Jiang, J., Li, X., Zheng, L. (2024). Adaptive and robust channel estimation for IRS-Aided millimeter-wave communications. IEEE Transactions on Vehicular Technology, 73(7): 9411-9423. https://doi.org/10.1109/TVT.2024.3385776
[18] Hongyun, C., Mengyao, Y., Xue, P., Ge, X. (2024). Joint active and passive beamforming design for hybrid RIS-aided integrated sensing and communication. China Communications, 21(10): 1-12. https://doi.org/10.23919/JCC.ja.2023-0213
[19] Zhou, G., Zhou, X., Li, W., Zhao, D., Song, B., Xu, C., Zhang, H., Liu, Z., Xu, J., Lin, G., Deng, R., Hu, H., Tan, Y., Lin, J., Yang, J., Nong, X., Li, C., Zhao, Y., Wang, C., Zhang, L., Zou, L. (2022). Development of a lightweight single-band bathymetric LiDAR. Remote Sensing, 14(22): 5880. https://doi.org/10.3390/rs14225880
[20] Gao, N., Huang, Q., Pan, G. (2024). Ultra-Broadband sound absorption characteristics in underwater ultra-thin metamaterial with three layer bubbles. Engineering Reports, 6(11): e12939. https://doi.org/10.1002/eng2.12939
[21] Lalithakumari, S., Danasegaran, S.K., Pandian, R. et al. Investigation of Octuplet Patch Terahertz Antenna for the Application of Breast Cancer Detection. Sens Imaging 26, 68 (2025). https://doi.org/10.1007/s11220-025-00587-5
[22] Hossain, M.N., Islam, M.A.A., Hossain, M.I. (2023). Design and performance analysis of defected ground slotted patch antenna for sub-6 GHz 5G applications. Journal of Engineering Advancements, 4(04): 130-140. https://doi.org/10.38032/jea.2023.04.004
[23] Renit, C., Ajith Bosco Raj, T. (2024). Wearable frequency selective surface-based compact dual-band antenna for 5G and Wi-Fi applications. Automatika: Journal for Control, Measurement, Electronics, Computing and Communications, 65(2): 454-462. https://doi.org/10.1080/00051144.2023.2296796
[24] Ullah, H., Cao, Q., Khan, I., Rahman, S.U., Jabire, A.H. (2023). A novel frequency selective surface loaded MIMO antenna with low mutual coupling and enhanced gain. Progress in Electromagnetics Research M, 118: 83-92. https://doi.org/10.2528/PIERM23040607

APPENDIX

1. Cost-Performance Tradeoff Analysis

1.1 Material cost breakdown

1.1.1 Baseline Antenna (Without FSS)

- FR4 substrate (25×25×1.6 mm): $0.18
- Copper cladding (0.035 mm): $0.12
- **Total Cost:** $0.30 per unit

1.1.2 FSS-Integrated Antenna

- Additional FR4 layer (125×125×1.6 mm): $1.05
- Additional copper for FSS pattern: $0.85
- Total Cost: $2.20 per unit (633% increase)

Cost estimates based on 2024 PCB fabrication quotes from JLCPCB and PCB Way for 100-unit batches as shown in Table A1.

Table A1. Performance vs. Cost Metrics

Configuration	Cost	Peak Gain	Gain Improvement	Cost per dB Gain Increase
Without FSS	$0.30	6.00dBi	-	-
3×3 FSS	$1.50	7.63dBi	+1.63dBi	$0.74/dB
5×5 FSS	$2.20	7.93dBi	+1.93dBi	$0.99/dB

2. Cost Optimization Findings

2.1 Nonlinear performance scaling

- The 5×5 FSS provides only 0.3 dBi additional gain over 3×3 (+19%) at 47% higher cost
- 3×3 configuration offers better cost/dB ratio (0.74 with 0.99)

2.2 Material analysis

Rogers RO4003C (εr=3.55) would increase cost 5× but only improve gain by ~0.5 dBi

2.3 FR4 provides optimal cost/performance for Sub-6 GHz applications

3. Volume Production Savings

- At 1,000 units, costs reduce by 30% due to panel utilization efficiencies
- Automated alignment reduces assembly time by 40% vs manual placement

4. Cost-Performance Tradeoffs

The selection of FR4 substrate and copper-clad construction was driven by rigorous cost-performance analysis. While the 5×5 FSS configuration achieves 7.93 dBi gain (32% improvement over baseline), the 3×3 FSS offers better cost efficiency at 0.74 per dB gain increase versus 0.99 for 5×5. This trade-off becomes particularly relevant for large-scale 5G deployments where thousands of units may be required.

Material alternatives were evaluated:

- Rogers RO4003C: +0.5 dBi gain at 5× cost
- Taconic RF-35: +0.7 dBi at 7× cost

The FR4 implementation maintains S_{11}<-15dB across all configurations while meeting industrial cost targets of <$3/unit at scale. For applications requiring >8dBi gain, hybrid FSS designs using partial Rogers substrates may be considered, as shown in Table A2.

Table A2. Cost-Performance Trade-offs of FSS Configurations

Design	Unit Cost	Ga in (dBi)	ΔGain	Cost/dB	BW (MHz)
No FSS	$0.30	6.00	-	-	400
3×3 FSS	$1.50	7.63	+1.63	$ 0.74	500
5×5 FSS	$2.20	7.93	+1.93	$ 0.99	500
RO4003C Hybrid	$4.80	8.20	+2.20	$ 1.75	525

4.1 Cost-performance comparison

(1) Industrial Viability
- FR4 accounts for 78% of 5G small cell antenna substrates (ABI Research 2023)
- Copper etching processes have >99% yield at 0.5mm trace widths

(2) Deployment Scenarios
- Urban high-density: 5×5 FSS justified for premium performance
- Rural coverage: 3×3 FSS provides optimal cost/performance

(3) Lifecycle Costs
- FR4 exhibits <0.5dB performance degradation over 5 years
- Comparable to Rogers substrates in accelerated aging tests

5. Thermal Analysis Methodology

5.1 Thermal expansion modeling

- Simulated thermal deformation of the FR4 substrate and copper FSS using **CST's Multiphysics Suite**.
- Parameters: Coefficient of Thermal Expansion (CTE) for FR4 (∼13–16 ppm/°C) and copper (∼17 ppm/°C).

5.2 Electromagnetic performance impact

- Shifts in **S_{11},** gain, and radiation efficiency across −20°C to 60°C.

5.3 Environmental chamber testing

- Measurement of S-parameters and gain of the fabricated prototype under controlled temperatures.

6. Key Results in relevant to thermal analysis

- **Thermal Drift of Resonant Frequency**
  - Shift due to ε_{sub} changes in FR4 (e.g., ±0.5% over the temperature range).
- **Structural Integrity**
  - Warping of the FSS array and its impact on unit-cell periodicity.

7. Performance Metrics

Gain variation (e.g., ±0.3 dBi) and S_{11sub} degradation (e.g., −15 dB to −12 dB at 60°C).

7.1 FSS-antenna alignment specifications (Table A3)

- **Optimal Spacing (H):**
  - The 23.4 mm gap between the antenna and FSS (Figure 4) is critical for phase coherence (Eq. 1).
  - **tolerance limits**: ±0.5 mm to maintain gain within 0.2 dBi of the peak value (7.93 dBi).
- **Alignment Accuracy:**
  - **Mechanical fixtures** (e.g., nylon spacers) ensures parallel alignment.
  - **Lateral misalignment** >2 mm degrades S_{11} by 1–2 dB (based on CST simulations).
- **Fabrication and assembly**
  - **Substrate Handling:** FR4 warping prevention: laser-cut alignment markers on the substrate edges.
  - **FSS Unit-Cell Precision:** Etching tolerance: ≤0.1 mm for copper traces to avoid resonant frequency shifts.
- **Mounting Recommendations:**
  - Non-conductive screws (e.g., PTFE) to minimize near-field distortion.

Table A3. Tolerances and performance impact

Parameter	Optimal Value	Tolerance	Performance Impact if Exceeded
FSS-Antenna Spacing	23.4mm	±0.5mm	Gain drop ≤0.2dBi
Lateral Alignment	Centered	≤2mm offset	S_{11} degradation 1-2dB
Unit-Cell Precision	25mm×25mm	±0.1mm	Frequency shift ≤50MHz

a) Thermal Cycling Tests (Table A4)
- **Standard:** IEC 60068-2-14 (Temperature cycling: −20°C to +60°C).
- **Procedure:**
  - Subject the prototype to **1000 cycles** (1 cycle = 30 min ramp, 30 min dwell).
  - Measure **S11, gain, and radiation efficiency** every 100 cycles.
  - <5% shift in resonant frequency (3.5 GHz) due to FR4 substrate aging.
  - Gain reduction <0.5 dBi after 1000 cycles.

Table A4. Aging test results vs. cycle count

Cycles	Gain (dBi)	S_{11}(dB)	Resonant Freq. Shift
0	7.93	−17.0	0 MHz
500	7.82	−16.2	+25 MHz
1000	7.65	−15.5	+45 MHz

***b) Humidity Exposure* (*Table A 5*)**
- **Standard:** IEC 60068-2-30 (Damp heat, 85% RH at 85°C for 500 hours).
- **Focus:** Corrosion effects on copper FSS and solder

joints.

Table A5. Proposed Compliance Test Items

Standard	Test Parameter	Target	Our Results	Compliance?
3GPP TR 38.901	Gain at 3.5 GHz	>7dBi	7.93dBi	Yes
FCC Part 27	OOBE at 4.0GHz	<−13dBm/MHz	−15.2dBm/MHz	Yes
IEEE 62704-3	SAR (1g avg.)	<1.6W/kg	1.2W/kg	Yes
ETSI EN 301 908-1	Bandwidth (n78)	≥100MHz	500MHz	Yes

7.2 Simulation-based reliability analysis

- **Material Degradation Modeling**
  - **ANSYS Sherlock** is used to predict FR4 delamination and copper oxidation over 5–10 years.
  - Correlate with experimental data.
- **Performance Projections:**
  - Simulate gain loss and S_{11} degradation under prolonged thermal stress.

7.3 Compliance with 5G standards

3GPP TR 38.901 (Channel Model for Sub-6 GHz)

- **Key Metrics:**
  - **Radiation Efficiency:** Target >80% (achieved: 82%).
  - **Peak Gain:** Meets 3GPP's recommendation of >7 dBi for urban microcells (achieved: 7.93 dBi).
  - **Impedance Bandwidth:** Covers **n78 (3.3–3.8 GHz)** with S11< −10 dB (500 MHz bandwidth).
- **Simulation Alignment:**
  - Validate radiation patterns against 3GPP's **clustered delay line (CDL) models** for urban scenarios.